Testing anomalous WWγ couplings in radiative charged current ep scattering

T. Helbig *

Deutsches Elektronen-Synchrotron DESY, Notkestrasse 85, D-W2000 Hamburg 52, Germany

H. Spiesberger **

*II. Institut für Theoretische Physik der Universität Hamburg, Luruper Chaussee 149,
D-W2000 Hamburg 50, Germany*

We study the possibility to measure the anomalous couplings κ and λ in the WWγ three-boson vertex at HERA and LEP×LHC using the process ep → $\nu\gamma$X. We discuss event distributions and their dependence on kinematical cuts in order to find observables with optimal sensitivity to the three-boson couplings. With an integrated luminosity of $\int dt \, \mathscr{L} = 10^3$ pb^{-1}, HERA will be able to establish 2σ limits of $\kappa = 1.0^{+1.9}_{-1.7}$ and $\lambda = 0^{+2.1}_{-1.8}$. At LEP×LHC the corresponding limits are smaller and comparable to those from single W production in neutral current ep scattering.

1. Introduction

In the standard model of electroweak interactions, the couplings of the charged W boson to its neutral partners, photon and Z boson, are unambiguously fixed by the non-abelian nature of the SU(2) × U(1) gauge symmetry. It is the aim of experiments in high-energy physics to test also this aspect of the standard model. In order to measure the three-boson couplings and to quantify possible deviations from the standard model, one has to generalize the standard model lagrangian and allow for some ad hoc introduced non-standard interaction. One possible and commonly used way is to release the restrictions imposed by SU(2) gauge symmetry and consider the most general Lorentz invariant three-boson interaction preserving electromagnetic U(1) gauge symmetry. Excluding C and P odd terms, two

anomalous couplings κ and λ can be introduced which are related to the magnetic dipole and the electric quadrupole moment of the W boson [*].

Couplings of this type can emerge e.g. in theories where the charged bosons are composite objects [1]. They are predicted also within the standard model framework as a result of radiative effects [2]. However, being of the order $O(\alpha/\pi)$, these standard model contributions to the anomalous couplings are presently (and in the near future) beyond observability.

The introduction of anomalous couplings violates unitarity. One consequence of this is, that radiative corrections cannot be calculated in a consistent way anymore. The approach followed here is a purely phenomenological one, therefore. In order to restore the unitarity cancellations of the theory one would have to introduce additional changes in the lagrangian. This would make the theoretical framework depending on a number of assumptions and model parameters. We do not find it suitable to complicate our analysis by this from the very beginning. However, if experiments would show that the data cannot be fitted with the standard model couplings, a more consistent theoretical framework would have to be used for the investigation of the phenomena.

In this paper we study the possibility to measure anomalous couplings of the WWγ vertex in radiative charged current scattering at HERA and LEP × LHC

$$e^- + p \rightarrow \nu_e + \gamma + X. \tag{1}$$

This process together with single W production

$$e^- + p \rightarrow e^- + W + X, \tag{2}$$

are those processes in deep inelastic electron scattering which have a potential to obtain information on the three-boson couplings of the W boson. The latter process was studied in ref. [3] (see also ref. [4]). It has the advantage of being a neutral current process whose cross section is enhanced by the $1/Q^2$ behaviour of the photon propagator. However, process (2) proceeds at HERA close to the kinematical threshold $y \geqslant M_W^2/S$ and $x \leqslant 1 - M_W^2/yS$ and, in addition to this, the number of events which can be used in an analysis is restricted by the need to identify the W by one of its leptonic decays. Both complications do not apply to (1). Rather the measurement of (1) is based on clean events characterized by a photon and missing transverse momentum. Therefore it is not obvious that (2) should be superior to (1). Moreover, process (1) is completely free from contributions of the ZWW couplings which enter in (2) as well, although being suppressed by the Z propagator.

---

[*] *C or P violating couplings are restricted by experiments on the neutron's electric dipole moment to be very small.*

There is an extensive literature on possible measurements of anomalous couplings in other processes. Recently, in ref. [5] the process $\nu_\mu p \rightarrow \mu \gamma X$, related to (1) by crossing, was studied. The potential of hadron colliders was investigated in ref. [6]. In e^+e^- annihilation there is a variety of processes with access to anomalous three-boson couplings [7]. Particularly interesting is $e^+e^- \rightarrow W^+W^-$ [8] where both the WWγ and the WWZ vertex enter already at the tree level and due to strong unitarity cancellations there is a considerable sensitivity to the three-boson couplings.

Future high-energy experiments like LEP II, SSC or LHC will certainly be able to measure anomalous couplings with much higher precision than can be expected from HERA. But since we will have to wait quite some time until these machines start operation, it is nevertheless interesting to know whether HERA could be able to improve present experimental bounds on anomalous WWγ couplings [9].

In sect. 2 we describe some general features of process (1). This will help us to find cuts which define the process from an experimental point of view and allow to use a simple Monte Carlo program for its simulation. In sect. 3 we present results for single differential cross sections and study in some more detail the influence of experimental cuts. There we also present 1σ and 2σ limits for the measurement of κ and λ at HERA and LEP × LHC. In sect. 4 we discuss some sources of uncertainties and background processes. The complete cross section formula is contained in appendix A.

2. Monte Carlo simulation of ep → νγX

Process (1) is described in the parton model by charged current electron–quark and electron–anti-quark scattering

$$e^- + q \rightarrow \nu_e + q' + \gamma,$$

$$e^- + \bar{q} \rightarrow \nu_e + \bar{q}' + \gamma. \tag{3}$$

We denote the momenta of the incoming (outgoing) lepton and quark by p_e (p_ν) and p_q (p_q'), that of the photon by k. The quark momentum p_q is a fraction x of the proton momentum P: $p_q = xP$.

The common deep-inelastic kinematic variables are defined with the help of the total hadronic final-state momentum P_X

$$Q^2 = -(P_X - P)^2, \qquad x = \frac{Q^2}{2P(P_X - P)}. \tag{4}$$

We emphasize that the final state photon momentum does not contribute to P_X. Q^2 and x can be measured e.g. by using the Jaquet–Blondel method [10]. Since we do, however, not use a Monte Carlo simulating the full hadronic final state, we concentrate in the following on the momentum of the scattered quark. Ignoring fragmentation and hadronization effects, its energy $E_{q'}$ and its polar angle $\theta_{q'}$ are identified with the energy and the polar angle of a separated jet. The assumption that a jet can be identified in the hadronic final state is justified if its transverse momentum (the transverse momentum of the scattered quark $p_T^{q'}$) is large enough. The final-state photon is characterized by its energy E_γ and its polar angle θ_γ. Both $\theta_{q'}$ and θ_γ are measured with respect to the proton beam. The description of the final state of process (3) is completed by an azimuthal angle ϕ which we chose as the angle between the transverse momenta of the photon and the scattered quark in a plane perpendicular to the beam.

The complete formula for the cross section of process (1) is given in appendix A for arbitrary anomalous couplings κ and λ. The typical features of the differential cross section are its infrared and collinear poles. In the vicinity of $E_\gamma \simeq 0$ and for configurations where the photon is parallel to either of the charged in- or outgoing fermions, the cross section is large and completely determined by the standard model couplings. The anomalous couplings enter in a diagram which is neither infrared nor collinear divergent. Deviations from the standard model predictions have therefore to be looked for in a phase space region where the photon is energetic and well-separated from both the incoming lepton and quark as well as from the scattered quark. This phase space region can be described by the following cuts:

A cut on the transverse photon momentum

$$p_T^\gamma = E_\gamma \sin \theta_\gamma \geqslant p_{T,\min}^\gamma, \tag{5}$$

is required for the photon being observable in the detector. Since for very large photon energies, condition (5) still allows small angles so that the photon could be lost in the beam pipes, we add a condition on the polar angle of the photon

$$\theta_{\gamma,\min} \leqslant \theta_\gamma \leqslant \theta_{\gamma,\max}. \tag{6}$$

Both cuts (5) and (6) guarantee the separation of the photon from the initial electron and quark.

To define the phase space region where the photon is isolated from the scattered quark (the current jet) we use the condition

$$R = \sqrt{\Delta\eta^2 + \phi^2} \geqslant R_{\min}, \tag{7}$$

on the distance in the rapidity–azimuthal plane. $\Delta\eta = \eta_\gamma - \eta_{q'}$ is the difference of rapidities of the photon and the scattered quark, $\eta_i = \frac{1}{2} \ln((1 + \cos \theta_i)/(1 -$

$\cos \theta_i$)). In practice one would apply a similar condition for the separation of the photon from hadrons in the final state.

In order to isolate the deep-inelastic kinematic regime where the parton model is applicable and in order to separate events whose kinematics can be analyzed in terms of a jet momentum, we have in addition to impose a cut on the transverse momentum of the hadronic final state

$$p_T^{q'} = E_{q'} \sin \theta_{q'} \geqslant p_{T,min}^{q'}. \tag{8}$$

Again, to ensure also for large energies $E_{q'}$ that the events be well contained in the detector, we add the condition

$$\theta_{q',min} \leqslant \theta_{q'} \leqslant \theta_{q',max}. \tag{9}$$

The cut on $p_T^{q'}$ implies

$$Q^2 \geqslant \frac{xS}{2} \left(1 - \sqrt{1 - \frac{4(p_{T,min}^{q'})^2}{xS}} \right), \tag{10}$$

and consequently

$$Q^2 > (p_{T,min}^{q'})^2. \tag{11}$$

Thus, the cut (8) guarantees that the parton model is indeed applicable if $p_{T,min}^{q'}$ is of the order of at least 1 GeV.

The charged current process is characterized by missing transverse momentum $\not{p}_T$. This property is used to separate the signal from radiative neutral current background by imposing a cut

$$\not{p}_T \geqslant \not{p}_{T,min}. \tag{12}$$

As a standard set of cut values we have chosen the following:

$$\left. \begin{array}{l} p_{T,min}^{\gamma} \\ \not{p}_{T,min} \\ p_{T,min}^{q'} \end{array} \right\} = \begin{cases} 10 \text{ GeV} & \text{for HERA} \\ 20 \text{ GeV} & \text{for LHC,} \end{cases}$$

$$\theta_{\gamma,min} = \pi - \theta_{\gamma,max} = 8°,$$

$$\theta_{q',min} = \pi - \theta_{q',max} = 8°,$$

$$R_{min} = 0.5. \tag{13}$$

For LEP × LHC where the center-of-mass energy is considerably larger than at HERA we use also the higher value of 20 GeV for the minimal transverse momenta but the same angular cuts and the same R_{min} for both machines. The beam energies are taken as $E_e = 30$ GeV, $E_p = 820$ GeV at HERA, $E_e = 50$ GeV, $E_p = 8$ TeV at LEPI × LHC, and $E_e = 100$ GeV, $E_p = 8$ TeV at LEPII × LHC. We also consider a possible upgrade of the HERA machine (denoted by HERA′) with $E_e = 35$ GeV, $E_p = 1200$ GeV. Throughout the paper, set 1 of Duke–Owens' parametrizations of the parton densities [11] are used with the scale chosen to be the hadronic momentum transfer Q^2. In the electroweak sector we take $M_W = 80.0$ GeV and $s_W^2 = 0.230$. Quark mixing is included, although its effect is negligible.

We developed a simple Monte Carlo program for the simulation of process (1). This program can be used as an event generator producing weighted events. Technical complications as arise for example in the calculation of the fully phase space integrated radiative cross section are avoided by the cuts described above. These cuts guarantee that events are produced only far away from both infrared and collinear poles. Therefore also all fermion masses could be neglected.

We checked this Monte Carlo by an independent program which was originally designed for the integration of the hard bremsstrahlung contribution to charged current radiative corrections [12]. In this latter program fermion masses had not been neglected, the phase space is described with a different set of kinematic variables, a different Monte Carlo integration routine was used, and also the calculation of the matrix element had been performed independently [13]. Results of this program had been compared with ref. [14] and agreement at the permille level had been found [12].

The two programs were applied to process (1) and have shown agreement within the statistical accuracy which was in most cases below 1% except in phase space regions where the cross section is extremely small.

3. Results

The total cross sections for various values of κ and λ with the cuts given in (13) are shown in table 1. According to these numbers, the measurement of anomalous three-boson couplings can be based on a sample of almost 300 events at HERA with $\int dt \, \mathscr{L} = 10^3$ pb^{-1}.

In the following we will first describe single differential cross sections with respect to angles and transverse momenta. This will give a more detailed overview over the characteristics of the process (1). From this we can justify our choice of cuts.

Fig. 2 shows the p_T^γ distribution for a set of values for κ (fig. 2a) and λ (fig. 2b) compared with the standard model result at $\kappa = 1$, $\lambda = 0$. The rapid increase of $d\sigma/dp_T^\gamma$ towards smaller p_T^γ is due to the infrared and collinear poles of the cross

κ	λ	$\sigma(\text{ep} \to \nu\gamma\text{X})/\text{pb}$
1	0	0.291
1	−2	0.292
1	−1	0.290
1	1	0.295
1	2	0.301
−1	0	0.319
0	0	0.303
2	0	0.283
3	0	0.279

section. Positive values of $\Delta\kappa = \kappa - 1$, and to a lesser extent negative λ, lead to smaller cross sections at moderate $p_T^\gamma \simeq 20$–50 GeV. At very large $p_T^\gamma > 80$ GeV, the deviations from the standard model result become large and non-standard values lead in general to a larger cross section. It is obvious that non-linear terms $\alpha \kappa^2$ and λ^2 are important. In this and the following figures, differences between different values for κ and λ are always significant: since for each event the weights have been calculated for the whole set of values for κ and λ, the differences $d\sigma(\kappa, \lambda)/dp_T^\gamma - d\sigma(\kappa = 1, \lambda = 0)/dp_T^\gamma$ are subject to statistical fluctuations small relative to themselves but not relative to the cross section $d\sigma(\kappa, \lambda)/dp_T^\gamma$.

The distribution with respect to the photon's polar angle, fig. 3, shows a maximum close to the direction of the proton beam. This maximum is due to a superposition of radiation of photons close to the directions of both the initial and the final state quark, the latter being deflected predominantly by small angles (see fig. 4). Note that the cut on R is included in this figure and photons parallel to the scattered quark are not allowed. The contribution of leptonic initial state radiation with $\theta_\gamma \simeq \pi$ is suppressed by the cut on p_T^γ. Fig. 3 shows that for a measurement of anomalous couplings events with small polar angles are especially important.

From the azimuthal distribution $d\sigma/d\phi$ in fig. 5 it can be seen that differences between non-standard values of κ and λ are visible almost in the whole range of ϕ
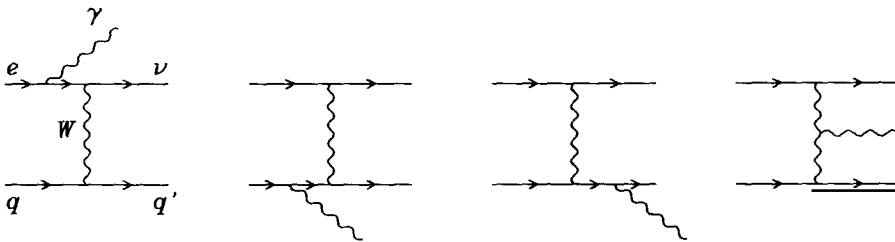

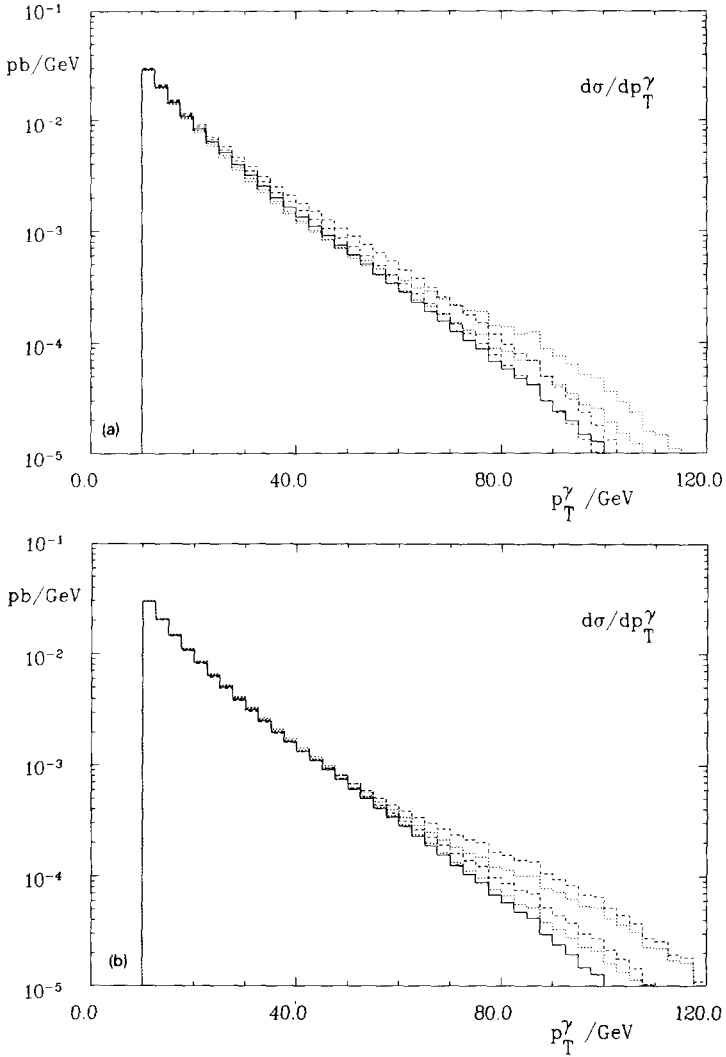Fig. 1. Feynman diagrams for the process $e + q \to \nu + \gamma + q'$.

Fig. 2. (a) Differential cross section $d\sigma/dp_T^\gamma$ at HERA ($S = 10^5$ GeV^2) with parameters and cuts as described in the text for $\lambda = 0$. The full line is for $\kappa = 1$ (i.e. for the standard model), the upper dotted line is for $\kappa = 3$, the lower dotted line for $\kappa = 2$, the upper dashed line for $\kappa = -1$, and the lower dashed line for $\kappa = 0$. (b) Same as (a) but now with parameters and cuts as described in the text for $\kappa = 1$. The full line now is for $\lambda = 0$ (i.e. for the standard model), the upper dotted line is for $\lambda = 2$, the lower dotted line for $\lambda = 1$, the upper dashed line for $\lambda = -2$, and the lower dashed line for $\lambda = -1$.

from 0 to π. This is very important for the measurement and the main reason why the sensitivity to anomalous couplings is not lost by the requirement that the photon has to be isolated. At small $\phi < 0.5$ ($\simeq 30°$), the effect of the cut on R is visible, whereas the dip at large ϕ is due to the cut on the missing transverse
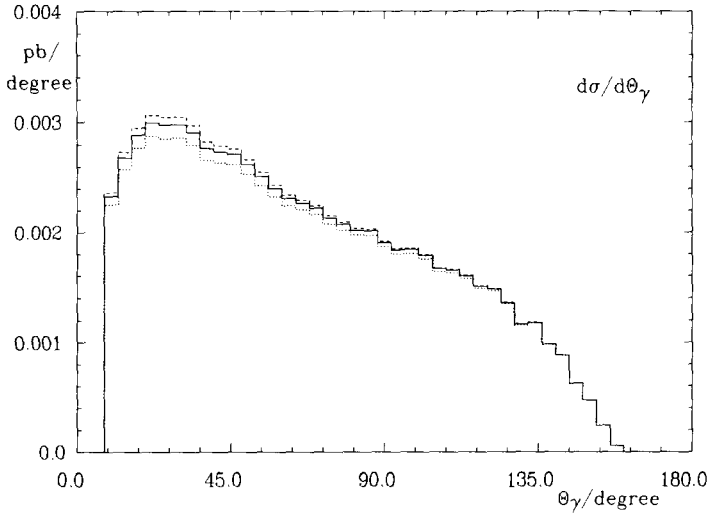
Fig. 3. Differential cross section $d\sigma/d\theta_\gamma$ at HERA ($S = 10^5$ GeV^2) with parameters and cuts as described in the text. The full line is for $\kappa = 1$, $\lambda = 0$ (i.e. for the standard model), the dotted line is for $\kappa = 2$, $\lambda = 0$, the dashed line for $\kappa = 1$, $\lambda = 1$.

momentum. The latter statement can be understood from the relation $\not{p}_T$
$= \sqrt{\left(p_T^\gamma + p_T^{q'} \cos \phi \right)^2 + \left(p_T^{q'} \sin \phi \right)^2}$. For $\phi = \pi$ one has $\not{p}_T = | p_T^\gamma - p_T^{q'} |$ and small values of $\not{p}_T$ would be possible if they would not be cut out.
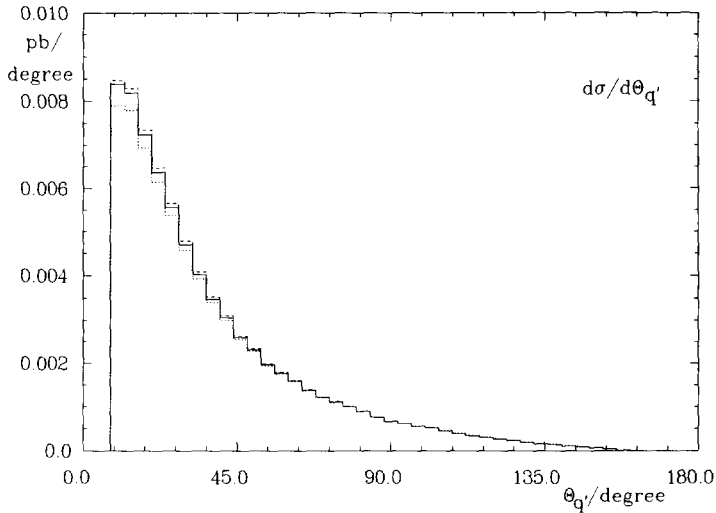

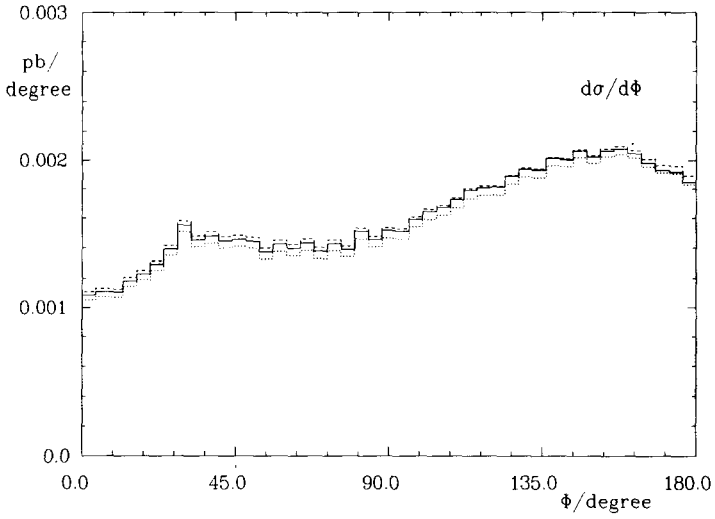Fig. 4. Differential cross section $d\sigma/d\theta_{q'}$ as in fig. 3.

Fig. 5. Differential cross section $d\sigma/d\phi$ as in fig. 3.

The information contained in figs. 3 and 5 is combined in fig. 6 which shows $d\sigma/dR$. It demonstrates that the sensitivity to κ and λ is obtained at relatively large values of R and is not reduced when cutting at the lower end of the spectrum. The events which are important for a measurement of the anomalous couplings are events with large R, i.e. events with well isolated photons. Above $R \simeq \pi$ the distribution shows a rapid fall-off. This is a consequence of the cuts on
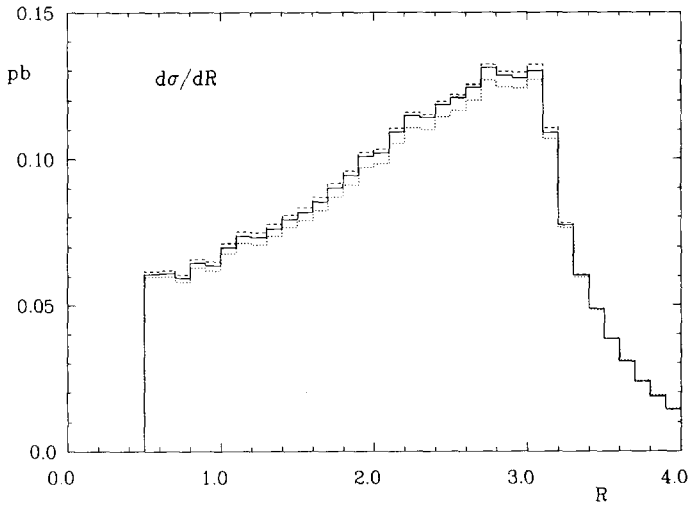
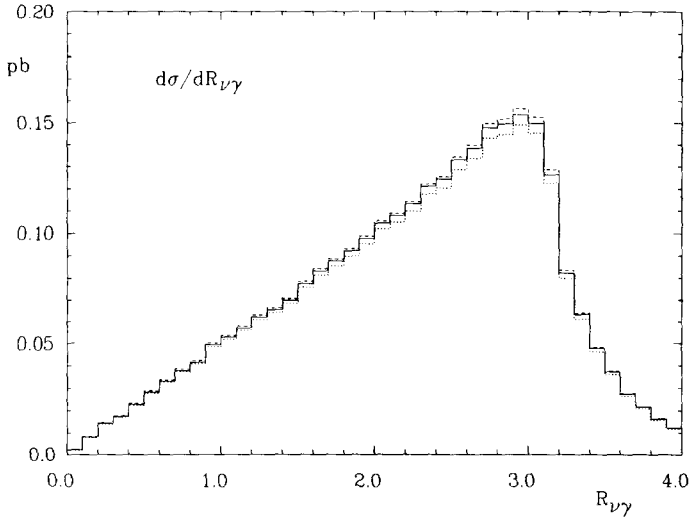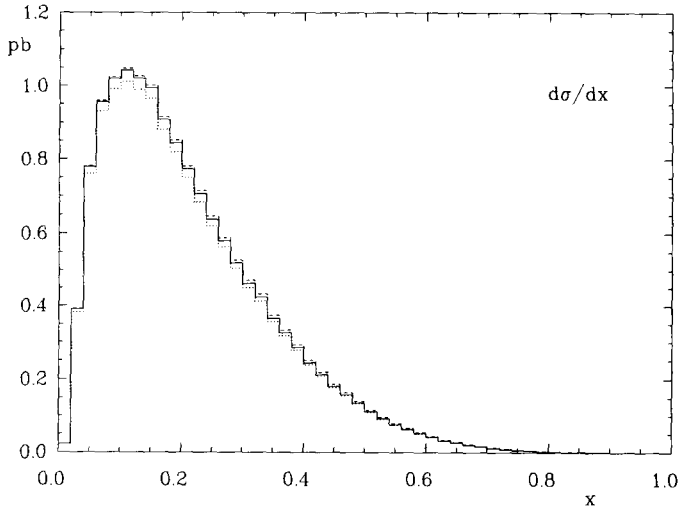Fig. 6. Differential cross section $d\sigma/dR$ as in fig. 3.

Fig. 7. Differential cross section $d\sigma/dR_{\nu\gamma}$ as in fig. 3.

$\theta_{q'}$ and θ_γ since values of $R \geqslant \pi$ can be reached only for large $\Delta\eta$ which in turn requires the photon and the scattered quark being close to the beams.

One might suspect that the phase space region where the photon is close to the outgoing neutrino is particularly sensitive to deviations from standard couplings. Since the neutrino has no charge, radiation into that direction is not enhanced by collinear poles. Differences in κ and λ could therefore show up as deviations from small standard model predictions. However, these configurations lead to smaller values for the missing transverse momentum and the cut on $\not{p}_T$, which is needed to reject the neutral current background, leads to a strong suppression in this phase space region. In fig. 7 we show the cross section differential with respect to the rapidity–azimuthal distance $R_{\nu\gamma} = \sqrt{(\eta_\nu - \eta_\gamma)^2 + (\phi - \phi_\nu)^2}$ of the photon and the missing momentum. It is seen that the cross section is dominated by configurations with large values of R_ν. From figs. 5 and 6 we conclude that the sensitivity on κ and λ is based on clean events which are characterized by large separations between the photon, the jet, and the missing momentum.
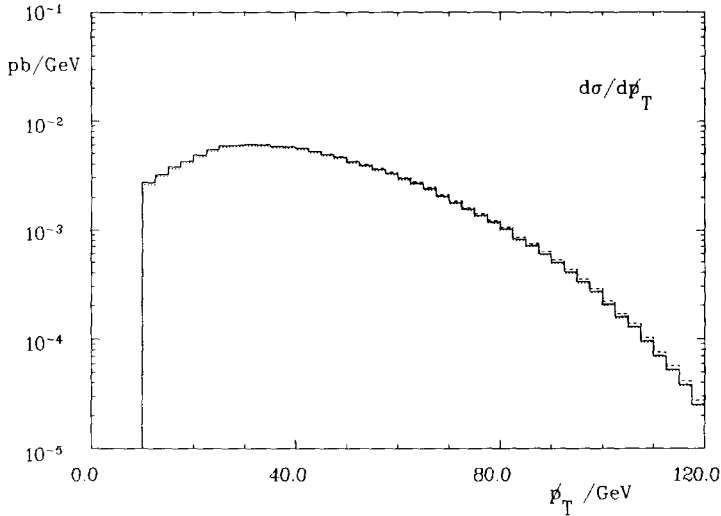
Finally, to complete the discussion of differential cross sections, we show in fig. 8 the x distribution which reflects the shape of the valence quark distributions. Sea quarks do not contribute much since small values of x are suppressed by the cut on $p_T^{q'}$. Therefore it is not essential for our purpose to use more recent parametrizations with improved low-x behaviour.

In fig. 9 we present the cross section differential with respect to the missing transverse momentum. It looks very similar to the distribution $d\sigma/dp_T^{q'}$. In spite of the cut (5), the photon does not contribute much to the p_T balance on the average.

Fig. 8. Differential cross section $d\sigma/dx$ as in fig. 3.

In order to study the sensitivity on anomalous couplings in a systematic way we consider the likelihood function L. It is defined by

$$L = \mathscr{S} \int d\xi \left\{ \left[\frac{d\sigma^{SM}}{d\xi} - \frac{d\sigma(\kappa, \lambda)}{d\xi} \right] - \frac{d\sigma(\kappa, \lambda)}{d\xi} \ln \frac{d\sigma^{SM}/d\xi}{d\sigma(\kappa, \lambda)/d\xi} \right\} \qquad (14)$$

Fig. 9. Differential cross section $d\sigma/d\not{p}_T$ as in fig. 3.

and is a measure for the probability that statistical fluctuations cause the observed distribution $d\sigma^{obs}/d\xi$ to coincide with the distribution $d\sigma(\kappa, \lambda)/d\xi$ predicted for a given set of values of κ and λ while the true distribution is $d\sigma^{SM}/d\xi = d\sigma(\kappa = 1, \lambda = 0)/d\xi$. ξ is any observable which can be constructed from the independent kinematic variables,

$$\frac{d\sigma}{d\xi} = \int d\sigma \; \delta\big(\xi - \xi(x, E_\gamma, \cos\theta_\gamma, \cos\theta_{q'}, \phi)\big), \tag{15}$$

and $\mathscr{I}$ is the integrated luminosity $\mathscr{I} = \int dt \; \mathscr{L}$.

From the above discussions of single differential distributions we conclude that the photon's transverse momentum p_T^γ should be the most promising candidate for ξ, since in $d\sigma/dp_T^\gamma$ differences for various values of κ and λ have been found to be most prominent. With this choice we studied the likelihood as a function of the values for the various cuts introduced in sect. 2. Fig. 10a shows L as a function of R_{min} and in fig. 10b we display L as a function of $\theta_{\gamma,min}$ for the two sets $\kappa = 2$, $\lambda = 0$ and $\kappa = 1$, $\lambda = 1$. Other cuts are kept at their standard values given in (13). We see that R_{min} can be chosen rather large without loosing sensitivity. This means that the photon isolation criterium does not restrict the potential for measuring κ and λ. In contrast to this, from fig. 10b it can be concluded that $\theta_{\gamma,min}$ should be small. A value of $\theta_{\gamma,min} = 30°$ would reduce the likelihood by a factor of about 2 as compared to L for our standard choice $\theta_{\gamma,min} = 8°$. Therefore it is essential for the measurement of anomalous couplings to be able to identify photons also in the forward direction close to the proton beam.

The cut values given in (13) have been determined from studying their influence on L in the same way, respecting of course constraints from detector properties. We found that reducing $p\!\!\!/_{T,min}$ below 10 GeV does not improve the sensitivity. The dependence of L on $p\!\!\!/_{T,min}$ is weak so that increasing its value to $p\!\!\!/_{T,min} = 20$ GeV would lead to a reduction of L of about 15% only, the precise value depending of course on κ and λ. The same is true for $p_{T,min}^{q'}$. For $\theta_{q',min}$ however, it is again desirable to choose a value as small as possible.

From studying the dependence of L on κ and λ we finally determine the 1σ and 2σ limits which can be reached at HERA and LEP × LHC. Here we used again the now justified set of cut values as given in (13). The results are collected in table 2. The 1σ (2σ) limits for $\Delta\kappa = \kappa - 1$ are obtained while keeping $\lambda = 0$ fixed and vice versa those for λ with fixed $\Delta\kappa = 0$. For both setups of HERA beam parameters we assumed an integrated luminosity of 10^3 pb^{-1}, whereas for LEPI × LHC we took 5×10^3 pb^{-1} and for LEPII × LHC 500 pb^{-1}.

The larger values for $\Delta\kappa(1\sigma)$ and $\Delta\kappa(2\sigma)$ at LEPII × LHC as compared to the lower-energy option LEPI × LHC are caused by the smaller luminosity at the former machine. For λ, the smaller luminosity is compensated by the higher energy. This behaviour is explained by the fact that terms containing λ have always
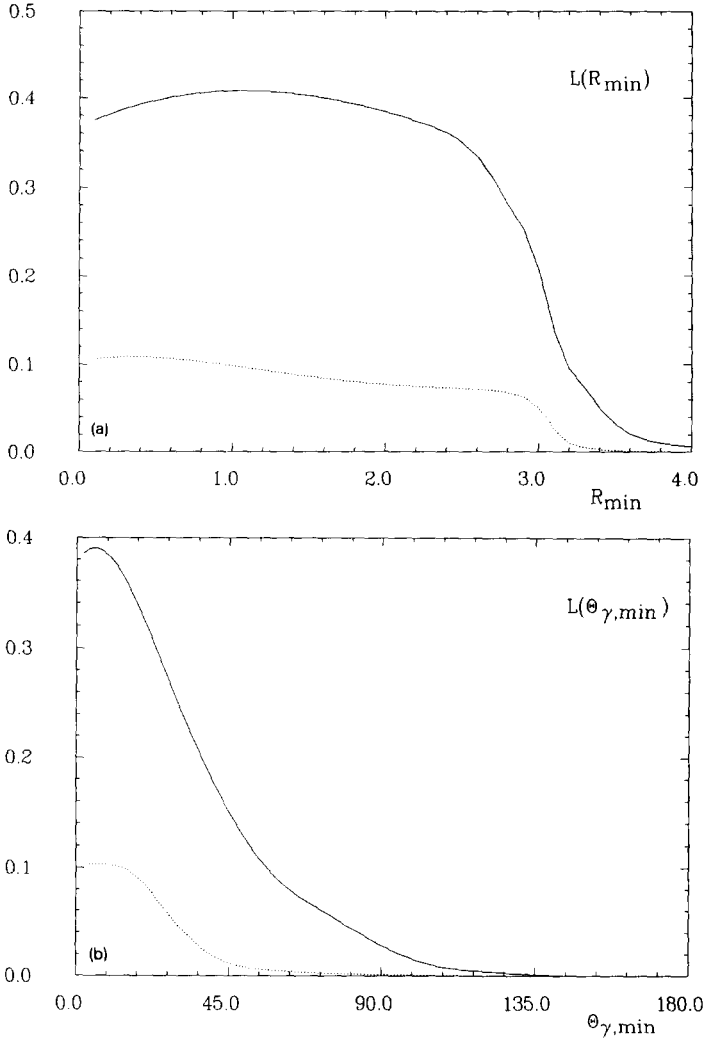
Fig. 10. (a) Likelihood L as a function of R_{min} at HERA ($S = 10^5$ GeV^2) for $\kappa = 2$, $\lambda = 0$ (full line) and $\kappa = 1$, $\lambda = 1$ (dotted line). (b) Likelihood L as a function of $\theta_{\gamma,min}$.

an additional factor $(p_1 p_2)/M_W^2$ ($p_{1,2}$ are any two of the particle's momenta) and thus grow more strongly with increasing energy than terms with κ.

Comparing these numbers with the results for single W production in neutral current ep scattering obtained in ref. [3], we find that the sensitivity of the process ep $\to \nu\gamma$X is worse by a factor of 2 to 3 for the lower-energy option of HERA. At larger center-of-mass energies, i.e. at LEP × LHC, the reach of both processes is comparable.

We should like to mention that the sensitivity of the measurement can in principal be improved if instead of a single differential distribution higher differen-

	HERA	HERA'	LEP I×LHC	LEP II×LHC
$\Delta\kappa(1\sigma)$	$+1.1/-1.0$	$+0.8/-0.7$	$+0.15/-0.15$	$+0.30/-0.31$
$\Delta\kappa(2\sigma)$	$+1.9/-1.7$	$+1.4/-1.3$	$+0.29/-0.30$	$+0.49/-0.52$
$\lambda(1\sigma)$	$+1.4/-1.1$	$+0.8/-0.6$	$+0.07/-0.04$	$+0.07/-0.06$
$\lambda(2\sigma)$	$+2.1/-1.8$	$+1.2/-1.0$	$+0.10/-0.08$	$+0.10/-0.09$

tial cross sections are used, since then more information enters into the analysis. Eq. (14) can accordingly be modified. It is therefore not excluded that a clever choice of binning in the 5-dimensional phase space could improve the 1σ and 2σ limits for κ and λ. One has, however, to take precautions that bins are not chosen too small such that the result could become sensitive to single events.

4. Discussion and conclusion

The measurement of κ and λ from the process ep $\to \nu\gamma$X as described in sect. 3 is based on the comparison of observed absolute event rates with theoretical predictions. It is therefore important to have a precise and complete knowledge of possible uncertainties entering in the calculation of the cross section as well as of possible background processes.

The main source of theoretical uncertainties for the cross section is our ignorance of a precise structure function input including higher order QCD corrections. By comparing two recent parametrizations of parton distribution functions from ref. [16] (sets B0 and B −) we found an uncertainty on the total cross section of 1.2%.

Higher order QCD effects can be estimated by studying the dependence on the scale μ^2 which is used in the parton distribution functions $q_f(x, \mu^2)$. We observed that the two choices $\mu^2 = Q^2$ and $\mu^2 = (p_T^{q'})^2$ lead to the largest differences in the cross section. The result for $d\sigma/dp_T^\gamma$ with these two possible choices is shown in fig. 11. The corresponding total cross sections differ by 1.3%. From fig. 11 it is seen that this difference occurs mainly at large p_T^γ since in this phase space region $(p_T^{q'})^2$ is in general considerably smaller than Q^2. The increase of $d\sigma/dp_T^\gamma$ in this region amounts to 10%. The measurement of the differential cross section at small photon transverse momenta, where the dependence on κ and λ is negligible, will certainly help to fix the normalization. However, the problem remains that higher-order QCD corrections could change the form of the differential cross sections. This calls for a study of QCD corrections to radiative charged current scattering.
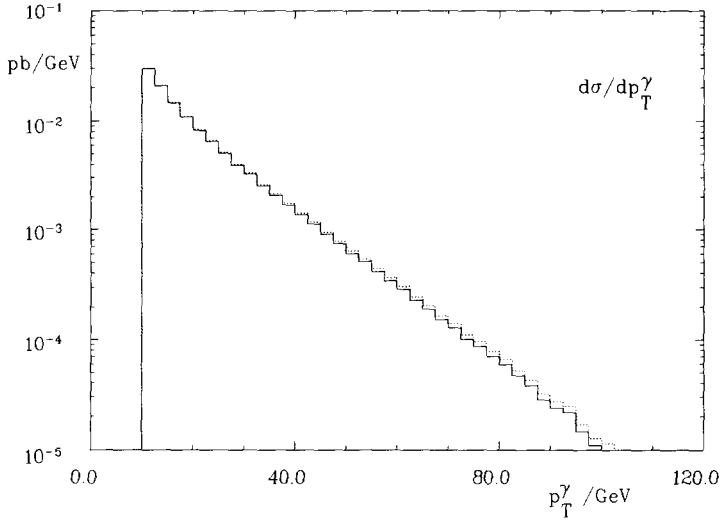
Fig. 11. Differential cross section $d\sigma/dp_T^\gamma$ at HERA ($\kappa = 1$, $\lambda = 0$) for two choices of the scale in the parton distribution functions. The full line is for $\mu^2 = Q^2$, the dashed line for $\mu^2 = (p_T^{q'})^2$.

There is a variety of processes which can lead to a photon in the final state. Among them there are the emission of photons during the fragmentation process of the final state quarks, hadronic decays, or π^0 misidentification. These backgrounds have still to be studied with the help of a complete Monte Carlo. From experience with other processes it can be expected that these sources are small if large energies and transverse momenta of photons are required.

Another possibly dangerous background is the radiative neutral current process $ep \to e\gamma X$ with missing transverse momentum caused by detector imperfections. The separation of NC and CC events by balance of the transverse momentum was studied in ref. [15]. From this reference we estimate the non-radiative NC background for $\not{p}_T \geqslant 10$ GeV to be of the order of 1 pb. Since we are considering a phase space region where no enhancement from infrared or collinear logarithms appears, one should expect that the radiative neutral current background is suppressed by a factor of $\alpha/\pi \simeq 2.3 \times 10^{-3}$. For an integrated luminosity of $\int dt$ $\mathscr{L} = 10^3$ pb^{-1} (corresponding to 5 years running with 200 pb^{-1}/y) this would lead to 2–3 events. Compared to the difference in the number of events for various sets of κ and λ that lead to a 1σ effect, this number is small but not negligible. The ratio of signal to background events could be improved by increasing the cut on $\not{p}_T$. Nevertheless, for a complete analysis a precise knowledge of the neutral current background is necessary.
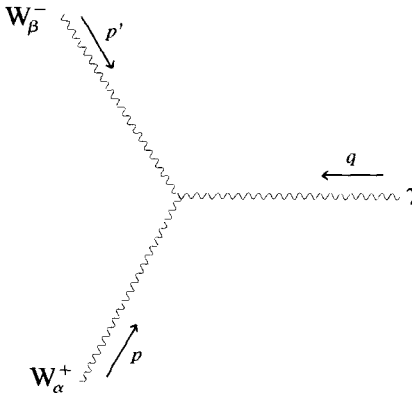
In conclusion, we have shown that radiative charged current scattering $ep \to \nu\gamma X$ is indeed sensitive to deviations of the three-boson couplings from their standard model values. HERA should be able to restrict the allowed values for $\Delta\kappa$ and λ

and the process considered in this paper can at least provide a valuable consistency check for results obtained from single W production in neutral current scattering as well as from other experiments.

Appendix A

Here we present the complete cross section formula for radiative charged current scattering with arbitrary κ and λ. Our convention for the WWγ vertex are [17]:

$$\Gamma_\mu = ie\{g_{\alpha\beta}(p - p')_\mu - g_{\alpha\mu}(p - q)_\beta$$

$$- g_{\beta\mu}(q - p')_\alpha + (\kappa - 1)(g_{\alpha\mu}q_\beta - g_{\beta\mu}q_\alpha)$$

$$+ \frac{\lambda}{M_W^2}[-g_{\alpha\beta}(p'q \cdot p_\mu - pq \cdot p'_\mu)$$

$$+ g_{\alpha\mu}(p'q \cdot p_\beta - pp' \cdot q_\beta)$$

$$- g_{\beta\mu}(pq \cdot p'_\alpha - pp' \cdot q_\alpha)$$

$$+ p_\mu p'_\alpha q_\beta - p'_\mu q_\alpha p_\beta]\}.$$

$$\text{(A.1)}$$

The resulting differential cross section reads

$$d\sigma(\text{ep} \rightarrow \text{e}\gamma X) = \frac{\alpha^3}{4\pi^2 S} \frac{1}{s_W^4} \frac{dx}{x} d^3 PS \left(\sum_{f=\text{u,c}} q_f \sum_{i,j=1}^{4} T_{ij} + \sum_{\bar{f}=\bar{\text{d}},\bar{\text{s}},\bar{\text{b}}} q_{\bar{f}} \sum_{i,j=1}^{4} \bar{T}_{ij} \right) \quad \text{(A.2)}$$

This formula is for unpolarized electrons. $S = (p_e + P)^2$, and q_f are the parton distribution functions. The 3-particle phase space can be parametrized by the

energy of the photon, the polar angles of the photon and the scattered quark, and by one azimuth

$$d^3 PS = \frac{\pi E_{q'} E_\gamma}{4 S_4} dE_\gamma \, d(\cos \theta_\gamma) \, d(\cos \theta_{q'}) \, d\phi \tag{A.3}$$

where

$$S_4 = E_e + x E_p - E_\gamma - (E_e - x E_p - E_\gamma \cos \theta_\gamma) \cos \theta_{q'} + E_\gamma \cos \phi \sin \theta_{q'} \sin \theta_\gamma. \tag{A.4}$$

E_e and E_p are the energies of the electron and the proton beam, respectively. The unobservable neutrino momentum and the overall azimuthal orientation has been integrated out. The quantities T_{ij} describe the products of Feynman diagrams for radiation from the initial lepton $(i = 1)$, from the initial quark $(i = 2)$, from the scattered quark $(i = 3)$ and from the intermediate charged W boson $(i = 4)$. The anomalous couplings contribute only in terms with i or $j = 4$. The T_{ij} depend on the 4-products of the particle momenta. We used

$$s = (p_e + p_q)^2, \qquad t = (p_e - p_\nu)^2, \qquad u = (p_e - p_{q'})^2,$$
$$\bar{s} = (p_\nu + p_{q'})^2, \qquad \bar{t} = (p_q - p_{q'})^2, \qquad \bar{u} = (p_\nu - p_q)^2, \tag{A.5}$$

and neglected fermion masses everywhere. As abbreviations for the W boson propagators we use

$$D = \frac{1}{t - M_W^2}, \qquad \bar{D} = \frac{1}{\bar{t} - M_W^2}. \tag{A.6}$$

In the following we list only the expressions for electron–quark scattering, those for electron–anti-quark scattering can be obtained by replacing $p_q \leftrightarrow -p_{q'}$ and consequently $s \leftrightarrow u$ and $\bar{s} \leftrightarrow \bar{u}$

$$T_{11} = \bar{D}^2 \frac{4 k p_q \bar{s}}{k p_e}, \tag{A.7}$$

$$T_{22} = D^2 Q_f^2 \frac{4 k p_e \bar{s}}{k p_q}, \tag{A.8}$$

$$T_{33} = D^2 Q_{f'}^2 \frac{4 k p_\nu s}{k p_{q'}}, \tag{A.9}$$

$$T_{12} = D\overline{D}Q_f \left[4\bar{s} - \frac{2s\bar{s}}{kp_e} - \frac{2s\bar{s}}{kp_q} + \frac{s^2\bar{s}}{kp_e kp_q} \right], \tag{A.10}$$

$$T_{13} = D\overline{D}Q_{f'} \left[\frac{s(\bar{s}-t)}{kp_e} + \frac{\bar{s}(\bar{t}-s)}{kp_{q'}} + \frac{kp_\gamma su}{kp_e kp_{q'}} - \frac{kp_q \bar{s}u}{kp_e kp_{q'}} + \frac{s\bar{s}u}{kp_e kp_{q'}} \right], \tag{A.11}$$

$$T_{23} = D^2 Q_f Q_{f'} \left[-\frac{kp_\gamma s\bar{t}}{kp_q kp_{q'}} + \frac{kp_e \bar{s}\bar{t}}{kp_q kp_{q'}} - \frac{s\bar{s}\bar{t}}{kp_q kp_{q'}} + \frac{\bar{s}(s-u)}{kp_{q'}} + \frac{s(\bar{u}-\bar{s})}{kp_q} \right], \tag{A.12}$$

$$T_{14} = D\overline{D}^2 \left[-4\kappa kp_q \bar{s} - s\bar{s} + \kappa s\bar{s} - \bar{s}t + t\bar{t} - u\bar{u} + \frac{(1+\kappa)kp_{q'} st}{kp_e} \right.$$

$$+ \frac{kp_\gamma s(\bar{s}-u-\kappa u)}{kp_e} + \frac{kp_q(t\bar{t} - 2\bar{s}t - \bar{s}u - u\bar{u})}{kp_e} + \left. \frac{s(2\bar{s}t - s\bar{s} - t\bar{t} + u\bar{u})}{2kp_e} \right]$$

$$+ D\overline{D}^2 \frac{\lambda}{2M_W^2} \left[\bar{s}t\bar{t} - s^2\bar{s} - s\bar{s}^2 - st\bar{t} + su\bar{u} + \bar{s}u\bar{u} \right.$$

$$- \frac{2kp_{q'} s\bar{s}t}{kp_e} - \frac{2kp_q \bar{s}tu}{kp_e} + 4kp_q(s\bar{s} + t\bar{t} - u\bar{u}) \right], \tag{A.13}$$

$$T_{24} = D^2 \overline{D} Q_f \left[-4\kappa kp_e \bar{s} - s\bar{s} + \kappa s\bar{s} - \bar{s}t + t\bar{t} - u\bar{u} + \frac{(1+\kappa)kp_\gamma s\bar{t}}{kp_q} \right.$$

$$+ \frac{kp_{q'} s(\bar{s}-\bar{u}-\kappa\bar{u})}{kp_q} + \frac{kp_e(t\bar{t} - 2\bar{s}t - \bar{s}u - u\bar{u})}{kp_q}$$

$$+ \left. \frac{s(2\bar{s}t - s\bar{s} - t\bar{t} + u\bar{u})}{2kp_q} \right]$$

$$+ D^2 \overline{D} Q_f \frac{\lambda}{2M_{W^2}} \left[\bar{s}t\bar{t} - s^2\bar{s} - s\bar{s}^2 - st\bar{t} + su\bar{u} + \bar{s}u\bar{u} \right.$$

$$- \frac{2kp_\gamma s\bar{s}\bar{t}}{kp_q} - \frac{2kp_e \bar{s}t\bar{u}}{kp_q} + 4kp_e(s\bar{s} + t\bar{t} - u\bar{u}) \right], \tag{A.14}$$

$$T_{34} = D^2 \overline{D} Q_{f'} \left[-4\kappa k p_\nu s + s\bar{s} - \kappa s\bar{s} + st - t\bar{t} + u\bar{u} - \frac{(1+\kappa) k p_e \bar{s} t}{k p_{q'}} \right.$$

$$\left. + \frac{k p_q \bar{s}(u - s + \kappa u)}{k p_{q'}} + \frac{\bar{s}(2s\bar{t} - s\bar{s} - t\bar{t} + u\bar{u})}{2 k p_{q'}} + \frac{k p_\nu (2s\bar{t} - t\bar{t} + su + u\bar{u})}{k p_{q'}} \right]$$

$$+ D^2 \overline{D} Q_{f'} \frac{\lambda}{2 M_W^2} \left[s^2 \bar{s} + s\bar{s}^2 - st\bar{t} + \bar{s}t\bar{t} - su\bar{u} - \bar{s}u\bar{u} \right.$$

$$\left. + \frac{2 k p_e s\bar{s}\bar{t}}{k p_{q'}} + \frac{2 k p_\nu s\bar{t}u}{\overline{k p}_{q'}} + 4 k p_\nu (s\bar{s} + t\bar{t} - u\bar{u}) \right], \tag{A.15}$$

$$T_{44} = D^2 \overline{D}^2 \left[4\kappa^2 k p_\nu k p_{q'} s + 4\kappa^2 k p_e k p_q \bar{s} - 4\kappa k p_{q'} st + 4\kappa k p_q \bar{s}t - 4\kappa k p_\nu s\bar{t} \right.$$

$$+ 4\kappa k p_e \bar{s}t + s^2 \bar{s} + s\bar{s}^2 + 2st\bar{t} + 2\bar{s}t\bar{t} - t^2\bar{t} - t\bar{t}^2 + stu$$

$$\left. + \bar{s}tu - t\bar{t}u + \bar{s}t\bar{u} + s t\bar{u} - t\bar{t}\bar{u} + tu\bar{u} + \bar{t}u\bar{u} + u^2\bar{u} + u\bar{u}^2 \right]$$

$$+ D^2 \overline{D}^2 \frac{\lambda}{M_W^2} \left[4\kappa k p_e k p_q (u\bar{u} - s\bar{s} - t\bar{t}) + 4\kappa k p_\nu k p_{q'} (u\bar{u} - s\bar{s} - t\bar{t}) \right.$$

$$+ k p_e \left(s\bar{s}^2 - 2s\bar{s}\bar{t} - \bar{s}^2\bar{t} + 3st\bar{t} - t\bar{t}^2 - s\bar{s}\bar{u} + s t\bar{u} + \bar{s}t\bar{u} - t\bar{t}\bar{u} - \bar{s}u\bar{u} + \bar{t}u\bar{u} + u\bar{u}^2 \right)$$

$$+ k p_q \left(s\bar{s}^2 - 2s\bar{s}t - \bar{s}^2 t + 3st\bar{t} - t^2\bar{t} - s\bar{s}u + stu + \bar{s}tu - t\bar{t}u - \bar{s}u\bar{u} + tu\bar{u} + u^2\bar{u} \right)$$

$$+ k p_\nu \left(s^2\bar{t} - s^2\bar{s} + 2s\bar{s}\bar{t} - 3\bar{s}t\bar{t} + t\bar{t}^2 + s\bar{s}u - s\bar{t}u - \bar{s}t\bar{u} + t\bar{t}u + su\bar{u} - \bar{t}u\bar{u} - u^2\bar{u} \right)$$

$$+ k p_{q'} \left(s^2 t - s^2\bar{s} + 2s\bar{s}t - 3\bar{s}t\bar{t} + t^2\bar{t} + s\bar{s}\bar{u} \right.$$

$$\left. -st\bar{u} - \bar{s}t\bar{u} + t\bar{t}\bar{u} + su\bar{u} - tu\bar{u} - u\bar{u}^2 \right) \right]$$

$$+ D^2\overline{D}^2 \frac{2\lambda^2}{M_W^4} \left[kp_q^2 \bar{s}tu + kp_\nu^2 s\bar{t}u + kp_{q'}^2 st\bar{u} + kp_e^2 \bar{s}\bar{t}\bar{u} \right.$$

$$+ kp_q kp_\nu u(s\bar{s} + t\bar{t} - u\bar{u}) + kp_e kp_{q'} \bar{u}(s\bar{s} + t\bar{t} - u\bar{u})$$

$$+ kp_q kp_{q'} t(s\bar{s} - t\bar{t} + u\bar{u}) + kp_e kp_\nu \bar{t}(s\bar{s} - t\bar{t} + u\bar{u})$$

$$\left. + kp_\nu kp_{q'}(s^2\bar{s} - st\bar{t} + 2\bar{s}t\bar{t} - su\bar{u}) + kp_e kp_q(s\bar{s}^2 + 2st\bar{t} - \bar{s}t\bar{t} - \bar{s}u\bar{u}) \right]. \quad (A.16)$$

For $\kappa = 1$ and $\lambda = 0$ these formulas agree with the standard model result for the hard bremsstrahlung cross section (see e.g. ref. [12]). The double pole terms proportional to the fermion masses m_i^2 can be neglected since they contribute only for small angles of the photon with respect to the fermion directions, but the corresponding phase space regions were excluded in our investigations by the cuts described in sect. 2.

We thank W. Buchmüller for helpful discussions.

Note added

While writing the manuscript of this paper we noticed that S. Godfrey has performed a similar study [18]. We disagree with his results on the p_T^γ distribution. Also our 1σ and 2σ limits for $\Delta\kappa$ and λ are not compatible with his 1σ and 2σ contours. Therefore we performed a number of additional checks of our program. In particular, as described already in the text, we checked our results with the help of the program of ref. [12] for the calculation of charged current radiative corrections to the process (1). This was possible with only minor changes. The latter program has already successfully been cross-checked with the independent calculation of ref. [14].

References

[1] M. Suzuki, Phys. Lett. B153 (1985) 289;
    T.G. Rizzo and M.A. Samuel, Phys. Rev. D35 (1987) 403
[2] W.A. Bardeen, R. Gastmans and B. Lautrup, Nucl. Phys. B46 (1972) 319;
    G. Couture and J.N. Ng, Z. Phys. C35 (1987) 65

[3] U. Baur and D. Zeppenfeld, Nucl. Phys. B325 (1989) 253
[4] M. Böhm and A. Rosado, Z. Phys. C42 (1989) 479
[5] G.V. Borisov and F.F. Tikhonin, Serpukhov preprint 90-64 (1990)
[6] J.D. Stroughair and C.L. Bilchak, Z. Phys. C26 (1984) 415;
    J. Cortes, K. Hagiwara and F. Herzog, Nucl. Phys. B278 (1986) 26;
    M. Kuroda et al., Nucl. Phys. B284 (1987) 271;
    U. Baur and D. Zeppenfeld, Nucl. Phys. B308 (1988) 127
[7] K. Hikasa, Phys. Lett. B128 (1983) 253;
    G.V. Borisov, V.N. Larin and F.F. Tokhonin, Z. Phys. C41 (1988) 287;
    E. Yehudai, Phys. Rev. D41 (1990) 33;
    G. Couture, S. Godfrey and R. Lewis, Carleton University preprint OCIP/C 91-3 (1991)
[8] C.L. Bilchak, R.W. Brown and J.D. Stroughair, Phys. Rev. D29 (1984) 375;
    M. Kuroda et al., Nucl. Phys. B284 (1987) 271;
    D. Zeppenfeld, Phys. Lett. B183 (1987) 380;
    K. Hagiwara, R.D. Peccei and D. Zeppenfeld, Nucl. Phys. B282 (1987) 253
[9] G.L. Kane, J. Vidal and C.P. Yuan, Phys. Rev. D39 (1989) 261, and references therein
[10] A. Blondel and F. Jaquet, ECFA Report Proc. of the Study of an ep facility for Europe, DESY
    79/48 (1979) p. 393
[11] D.W. Duke and J.F. Owens, Phys. Rev. D30 (1984) 49
[12] H. Spiesberger, Nucl. Phys. B349 (1991) 109
[13] M. Böhm and H. Spiesberger, Nucl. Phys. B304 (1988) 749
[14] D.Yu. Bardin, C. Burdik, P.Ch. Christova and T. Riemann, Z. Phys. C44 (1989) 149
[15] G. Ingelman, D. Notz and E. Ros, in Proc. HERA Workshop, Hamburg 1987, ed. R.D. Peccei,
    Vol. 1, p. 19
[16] J. Kwiecinski, A. Martin, R. Roberts and J. Stirling, Phys. Rev. D42 (1990) 3645
[17] K.J.F. Gaemers and G.J. Gounaris, Z. Phys. C1 (1979) 259;
    K. Hagiwara et al. Nucl. Phys. B282 (1987) 253
[18] S. Godfrey, Carleton University preprint OCIP/C 91-2 (1991)